

## VOID FRACTION AND RECONDENSATION RATE IN SUBCOOLED FORCED CONVECTIVE BOILING WITH FREON R 12

G. Stängl and F. Mayinger  
European Patent Office, Munich, Germany  
T. U. Munich, Germany

### ABSTRACT

This paper presents an investigation and results of volumetric void fraction and recondensation of bubbles in forced convective subcooled boiling. Dichlorodifluormethane ( $\text{CCl}_2\text{F}_2$ ) served as test fluid. The data were taken at different heat fluxes in a 12- to 25- bar pressure range, the mass fluxes have been varied from 500 to 3000  $\text{kg/m}^2\text{s}$  with an inlet subcooling in a range of 10 to 50K. The experiments have been conducted in an annular test channel with an 0.016m inner diameter and an 0.03m outer diameter. The inner tube of the annulus was heated by direct current. The void fraction data were gauged with a gamma - densitometer and a specially designed impedance void meter. The experimental results reveal that the void fraction is nearly constant from the onset of nucleation boiling to a subcooling of about  $\Delta T = 10\text{K}$ . A method for predicting the void fraction based on the drift flux model was calculated. With the help of this equation, a model for the recondensation rate could be derived and will also be presented in this paper.

### INTRODUCTION

The knowledge of the onset of nucleate boiling, void fraction, and pressure drop in subcooled boiling is important for the practical layout and design of liquid-cooled heat-generating systems operating with high heat fluxes. The phenomena occurring during subcooled boiling are explained in Figure 1. A fluid, which is subcooled at the channel inlet, flows through an uniformly heated tube. Because of the single-phase convective heat transfer, a superheated thermal boundary layer is established near the heated wall. Here, in small cavities, the first nucleation sites are activated and the first bubbles are generated ( $z_{nb}$ ). This phenomenon is called "onset of nucleate boiling" (ONB). The average bulk temperature at ONB is still

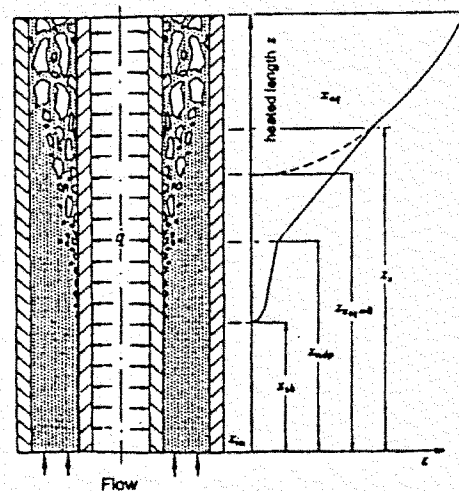


FIG. 1 VOID FRACTION DEVELOPMENT

considerably below the saturation temperature, and the generated bubbles are small and therefore condense as soon as they come in contact with the subcooled bulk flow. Consequently, the void fraction is very low in this region. The average bulk temperature increases with increasing channel length. Therefore, the bubble condensation rate decreases and the bubbles grow, tend to retreat from the heated wall, and drift into the bulk flow ( $z_{reco}$ ). Beyond the latter point the temperature near the center of the tube is still below the saturation temperature, and thermodynamic non-equilibrium continues to exist until this temperature reaches saturation ( $z_s$ ). Beyond that point, the released heat contributes only to liquid evaporation. Point  $z_{reco}$  reveals the saturation temperature of the flow when the first law of thermodynamic is applied neglecting the thermodynamic non-equilibrium. In subcooled boiling, not only the heat transfer

coefficient increases in comparison to single-phase flow, but also the void fraction, which causes a change of the fluid dynamic characteristics, such as the pressure drop. More detailed information concerning subcooled boiling can be found in [1]. Subcooled boiling phenomena have been investigated by several authors. Dix [2] and Jain et al. [3] have experimented in the region  $x_{eq} - x_{eq}$  using Freon 113 as test fluid, and Rouhani [4] using water, all of them, however, have worked in low-pressure ranges.

### EXPERIMENTAL SETUP

The experiments are conducted in a closed loop made of stainless steel. The loop is designed to operate with refrigerant 12 up to the critical pressure (41.6 bar). A vertically arranged test section having an annular cross section with a hydraulic diameter of 0.014 m is mounted in the loop. The inner tube consists of three sections. The unheated sections at the inlet and outlet are made of copper, the heated section is a stainless steel tube with a 16-mm outer diameter and a 1.5-mm wall thickness. This tube is supplied by direct current to guarantee uniform heat flux. The void fraction was gauged by means of a  $\gamma$ -densitometer and specially designed impedance probes. More detailed information of the test loop and the respective measuring devices have been published in [5].

### VOID FRACTION IN SUBCOOLED BOILING

As an example of the experimental results concerning the void fraction Fig. (2) shows the volumetric void fraction plotted over the local subcooling, which in this case is more revealing than the equilibrium quality defined below. This drawing illustrates the volumetric void fraction formation under different pressures. It is obvious that the void fraction decreases under increasing pressure. The overall behaviour of the void fraction can be explained by a combination of physical phenomena. The recondensation rate decreases with reduced subcooling of the liquid. Therefore the void fraction increases. On the other hand, the bubbles are able to detach from the heated wall and move inward to the bulk flow. This will be supported by even very little pressure differences due to the radial

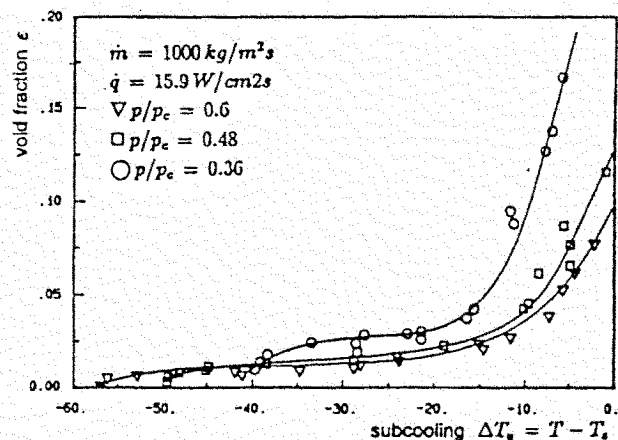


FIG. 2 VOID FRACTION FORMATION AT DIFFERENT PRESSURES

velocity differences in the flow. The differences in density will make the detached bubbles faster than the liquid flow surrounding them. This phenomenon is effected by decreasing the local void fraction gauged with the impedance probes. This behaviour of the void fraction at various mass fluxes can be explained by the decreasing radius of the bubbles and decreasing thickness of the boundary layer with increasing pressure. Therefore the bubbles detach later from the heated wall and condense more rapidly in the subcooled bulk flow, due to the smaller diameter and the smaller density difference between the phases.

The influence of the mass flux density on the void fraction formation is shown in Fig. (3). Within these test runs, pressure and heat flux were kept as constant as possible, the tests were however, performed with different mass fluxes. In this case, the void fraction is plotted over the equilibrium quality  $x_{eq}$  defined by eq. 1 :

$$x_{eq} = \frac{h_f - h_d}{h_{fg}} = \frac{c_p [T(x) - T_d]}{h_{fg}} \quad (1)$$

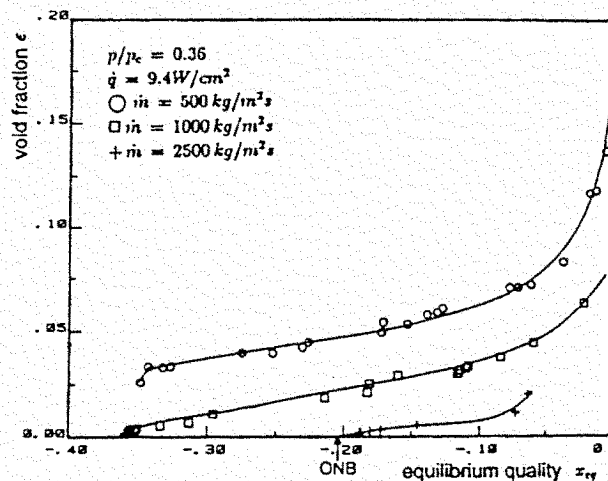


FIG. 3 VOID FRACTION FORMATION AT DIFFERENT MASS FLUX DENSITIES

The expected behaviour of the void formation, decreasing void fraction by increasing mass flux can be physically explained with the decreasing thickness of the superheated or saturated boundary layer. This leads to an earlier condensation of the bubbles attached at the wall. Moreover, the single phase heat transfer between the wall and the liquid increases with increasing mass flux and consequently, the walls super heating necessary for the bubble growth will be reached in lower subcooling ranges. The arrow marked with ONB indicates the onset of nucleate boiling calculated with the equation published by Bräuer [6]. The calculated value of the equilibrium quality for the ONB and the measured value are in a very good agreement. (i. e.  $x_{eq,cal} = 0.209$ ,  $x_{eq,meas} = 0.19$ ).

The changes in the void fraction formation by various heat flux densities is illustrated in Fig. 4. In this figure, only subcoolings up to  $\Delta T = -40$  [K] are shown, due to limitation of the test loop. The pressure and mass flux are kept constant. An interesting detail in this figure is the slight decrease of the void fraction measured with a heat flux of  $\dot{q} = 3.8$  [W/cm<sup>2</sup>]. As set out above, this can be explained with the detaching and floating of the bubbles in the bulk flow.

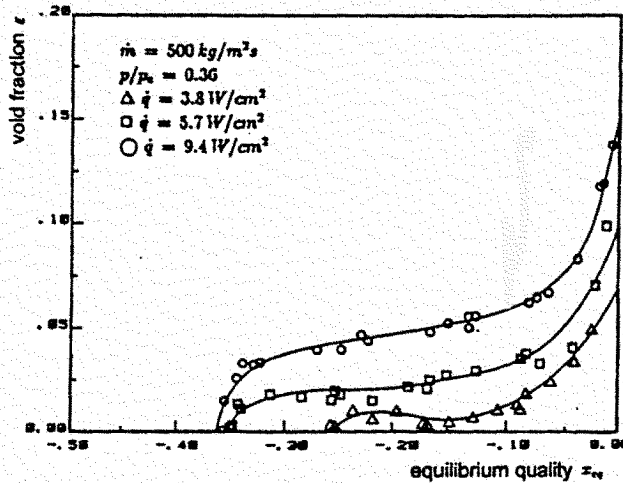


FIG. 4 VOID FRACTION FORMATION AT DIFFERENT HEAT FLUX DENSITIES

Moreover, due to the detaching of the bubbles, the turbulence in the boundary layer is increased which supports the heat transfer between the heated wall and the single phase liquid flow. Rouhani [4, 11] proved this physical phenomenon experimentally.

#### Modelling of the results

To calculate the true quality  $\dot{x}$ , defined by eq. 2

$$\dot{x} = \frac{\dot{M}_g}{\dot{M}} \quad (2)$$

with the total mass flow ( $\dot{M}$ ) and the vapor mass flow ( $\dot{M}_g$ ) can be calculated by using an energy balance. In this case, the measured radial temperature profile must be corrected. To fit the data, the well-known drift flux model, proposed by Zuber and Findlay [7], is used. In this model, the relationship between the volumetric void fraction  $\epsilon$  and the true quality  $\dot{x}$  is given by eq. 3

$$\epsilon = \frac{\dot{x}/\rho_g}{C_0 [\dot{x}\rho_g + (1 - \dot{x})/\rho_l] + V_{jg}/\dot{m}} \quad (3)$$

where  $V_{jg}$  is the vapor drift velocity and  $C_0$  is the distribution parameter. The drift velocity was set to

$$V_{jg} = 1.18 \left[ \frac{\sigma g (\rho_l - \rho_g)}{\rho_l^2} \right]^{0.25} \quad (4)$$

with the surface tension ( $\sigma$ ) and the acceleration due to gravity ( $g$ ). Using a stepwise regression analysis of about 500 data, measured in the above-described test section and the saturation data published by Friedel [8], the distribution parameter  $C_0$  was fit to

$$C_0 = \epsilon \left[ 1 + 1.049 Fr^{-0.885} (1 - J_0)^{0.164} \frac{p_s}{\rho_l} \left( \frac{1 - \dot{x}}{\dot{x}} \right)^{0.264} \left( 1 - \frac{p}{p_s} \right)^{0.124} \right] \quad (5)$$

with the average volumetric flow concentration  $\bar{\epsilon}$  defined by

$$\bar{\epsilon} = \frac{1}{1 + [(1 - \dot{x})/\dot{x}] (\rho_g/\rho_l)} \quad (6)$$

In consideration of the geometry and the mass flux, the Fround number:

$$Fr = \frac{\dot{m}^2}{g d_{hy} \rho_l^2} \quad (7)$$

was included. To indicate the degree of subcooling, i.e., the inlet subcooling of the fluid, a modified Jacob number was inserted, which is defined by

$$Ja = \frac{h_d - h_s}{h_{lg}} \quad (8)$$

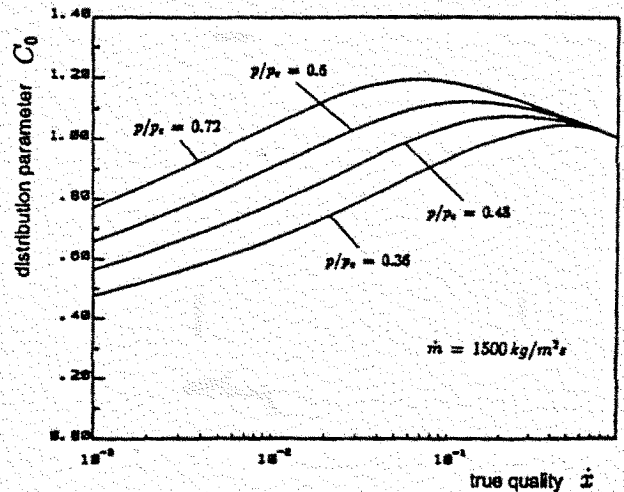


FIG. 5 CALCULATED DISTRIBUTION PARAMETER  $C_0$

Figure 5 shows the calculated distribution parameter  $C_0$  for a mass flux density  $\dot{m} = 1500$  [kg/m<sup>2</sup>s] at various pressures. Figure 7 illustrates the measured quality  $\dot{x}$ , gauged at the mass rate  $\dot{m} = 500$  [kg/m<sup>2</sup>s] at several heat flux densities and pressures, which is plotted versus the volumetric void fraction. The lines indicate the calculated void fraction with eq. (3) using the distribution parameter calculated with eq. (5). The data of refrigerant 12 under subcooled conditions ( $T < T_s$ ) and a pressure range  $12 \leq p \leq 40$  [bar] are regarded in eq. (4). The subcooling is limited by  $50 \leq \Delta T \leq 0$  K.

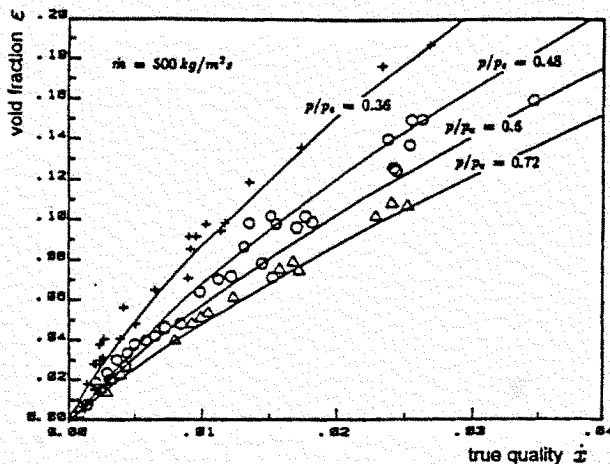


FIG. 6 TRUE QUALITY AND VOID FRACTION AT DIFFERENT PRESSURES

The mean deviation between the measured values and the prediction with the presented calculation method is 12%.

**Model of Recondensation**

Now, the true quality at hand, it is possible to determine the mass flow of the void which has recondensated due to the thermodynamic non-equilibrium. Models for the recondensation rate had been published by Ulrych [9], Dix [2], Huges [10] and Rouhani and Axelsson [11] and other. They all used slightly different approaches to calculate the recondensation rate. The model which is to be demonstrated here is based on a macroscopic view of the void fraction of subcooled boiling processes. Based on the conception that the present true quality can be obtained from the difference of the theoretically formed void bubbles in the boundary layer of the heated wall and the recondensated bubbles, the eq. 10

$$\dot{M}_g = \dot{M}_{g,theo} - \dot{M}_{rc} \tag{9}$$

can be used. If the theoretical void mass flow can be determined, the fraction of recondensation can be obtained by the present void mass flow received by the measured values. This theoretically formed steam amount can be determined by the eq. 10

$$\dot{Q}_{tot} = \dot{Q}_v + \dot{Q}_{sp} + \dot{Q}_{mc} + \dot{Q}_{co} \tag{10}$$

using the energy balance of the boundary layer (see Fig. 6). In this equation  $\dot{Q}_v$  stands for the heat flow which is used for the evaporation of the saturated or overheated fluid, which can be found at the heated wall or in the boundary layer.  $\dot{Q}_{sp}$  is the heat flow transferred by single-phase forced convection and  $\dot{Q}_{mc}$  is the heat flow transferred by micro-convection.  $\dot{Q}_{co}$  is the heat flow which is transferred by condensation at the bubble top/head to the subcooled fluid. This fraction of the total transfer of heat flow is small compared

to the heat flow which is transferred by micro-convection and can therefore be neglected according to Forster and Greif. This means that equation 10 can be simplified to

$$\dot{Q}_{tot} = \dot{Q}_v + \dot{Q}_{sp} + \dot{Q}_{mc} \tag{11}$$

The term micro-convection designates the disturbance of the boundary layer by detaching void bubbles letting subcooled fluid enter the boundary layer. The detaching bubble pulls some fluid from the boundary layer along in addition to its volume. A schematic representation of this process can be seen in fig. 6. This method of balancing the various heat transfer mechanisms is analogous to that of Rouhani [4, 11]. To simplify the calculation of the individual heat flows, the following assumptions are made:

- the boundary layer has saturation temperature (compare Larsen and Tong [12])
- the subcooled fluid has the same temperature level. This simplification was also used by Larson and Tong [12].

With these assumptions the various heat flows in equation 12 can be determined as follows. The heat flow which contributes to the evaporation of the fluid is described by eq. 12

$$\dot{Q}_v = \dot{M}_{g,theo} h_{fg} \tag{12}$$

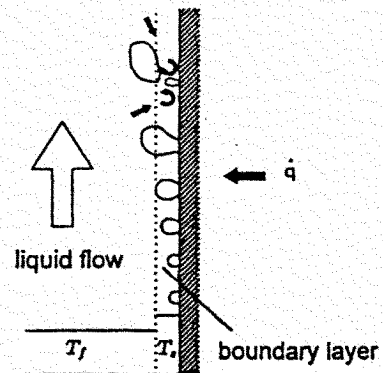


FIG. 6 SCHEMATIC ILLUSTRATION OF THE MICROCONVECTION

and contains the theoretically formed void mass flow  $\dot{M}_{g,theo}$ , which is required later to determine the recondensating void mass flow.

The heat flow  $\dot{Q}_{mc}$  transferred by micro-convection can be described by the equation 13

$$\dot{Q}_{mc} = B \dot{V}_{Bu} \rho_f (h_{f,s} - h_f) \tag{13}$$

according to Bowring [13]. The empirical factor B takes account of the mass of the fluid which follows at the immediate condensation of the bubble at the heated wall, respectively after the void bubbles have detached from the subcooled area. Hun and Griffith [14] have determined this factor to the value two by photographic measurements and theoretical considerations of this process, i.e. when a void bubble detaches from the heated wall, not only the volume of the void bubble is displaced by the subcooled fluid, but saturated, respectively overheated, fluid is drawn along with the bubble from the boundary layer. This process in subcooled boiling activities is also significant for the heat transfer. Using the before mentioned assumptions the growth of a bubble leads to a displacement of saturated fluid from the boundary layer into the subcooled fluid. With these assumptions the factor B was determined to three.

The heat flow  $\dot{Q}_p$  transferred by single phase forced convection was determined using the well-known equation by Colburn. It was applied by Rouhani in this rather unconventional form and presented more precisely in [1].

According to this relation the single phase heat transfer coefficient  $\alpha_{sp}$ , in this case between the saturated boundary layer and the subcooled fluid flow in the boiling channel, can be determined by eq. 14.

$$\alpha_{sp} = 0.023 \dot{m} c_p Pr^{(-2/3)} Re^{-0.2} \quad (14)$$

The transferred heat flux density by the single phase force convection can thus be obtained by eq. 15

$$\dot{q}_{sp} = \alpha_{sp}(T_s - T_f) \quad (15)$$

After having filled in the various heat fluxes and the algebraic transformation one receives an equation (which is equal to eq. 16 except the limits of the integral) for the recondensated void mass flow in a control element of the length  $\Delta z$ . Due to the differences in physical properties, surface tension and evaporation enthalpy, between water and the R12 used in this experiment, a strict distinction between the range where the bubbles adhere to the wall and the area of detaching bubbles cannot be made. Pictures with a high speed camera, as shot by Bräuer [6], reveal that the void bubbles detach very soon after boiling begin. Responsible for this early detachment is the considerably lower surface tension of R12 as compared to water. Therefore, this equation can be written integrally from the beginning of the bubble formation (ONB)  $z_b$  to the point  $z$ , where the fluid temperature equals the saturation temperature, as follows:

Using this equation the proportion of the recondensated void can be determined within the limits of predetermined assumptions. The results of the calculation of the recondensation rate are to be shown as an example in fig. 7. Here the void fraction and the recondensating void mass flux acc. to eq. 16 are drawn above the subcooling range  $\Delta T$ .

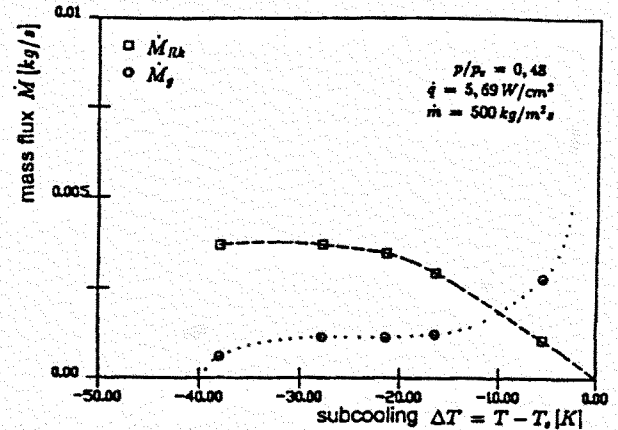


FIG. 7 EXISTING AND RECONDENSED VAPOR

The mass flux of the void  $\dot{M}_g$  present in the balance volume with the length  $\Delta z$  at a given subcooling temperature describes an almost horizontal line after its steep rise following the onset of boiling, as does the volumetric void fraction with which it is connected. At a subcooling rate of approx.  $\Delta T_s = -15 K$  it begins to increase exponentially. The recondensated void flux (acc. to eq. 16) shows a similar behaviour but decreases to the value 0 when reaching saturation temperature. This behaviour can be explained physically by the void bubbles' early detachment, due to the relatively low surface tension. Recondensation is highly determined by the fluid temperature, i.e. the bubble condensate faster at a high subcooling than at a low one letting a great proportion of the developed void condensate again after the onset of boiling. When subcooling decreases the bubbles in the fluid flow can exist longer and the

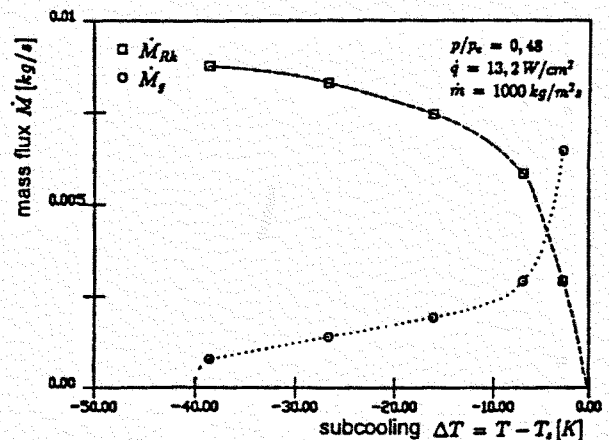


FIG. 8 EXISTING AND RECONDENSED VAPOR

present void flux increases proportionally, or resp. the recondensating void flux decreases until this process stops completely when reaching saturation temperature.

Fig. 8 shows the course of the recondensating mass flux at a higher

$$\dot{M}_{rc} = \int_{z_{sb}}^{z_s} \frac{[\dot{q} U_{heat} - \alpha_{sp}(U_{heat} \cdot 2\delta / (T_s - T_f(z)))z + \dot{m} A x(z) h_{fg}}{h_{fg} + B \rho_f(z) c_p(z) (T_s - T_f(z))} dz \quad (16)$$

heating performance and a higher mass flux density. This behaviour lets us conclude that the bubbles already condensate at the beginning of the heated course and not only at the boiling surface, but can detach from the surface of the inner tube and condensate in the subcooled fluid. These figures show that eq. 16 represents for the physical processes of recondensation under subcooled boiling to a high degree and allows the calculation of the recondensation with a known existing true quality.

#### NOMENCLATURE

|            |  |
|------------|--|
| $A$        | area [ $m^2$ ]                                     |
| $c_p$      | specific heat capacity of the liquid [ $kJ/kg K$ ] |
| $C_0$      | distribution parameter                             |
| $d_h$      | hydraulic diameter [ $m$ ]                         |
| $Fr$       | Froude number                                      |
| $g$        | gravity acceleration [ $m/s^2$ ]                   |
| $h$        | specific heat [ $kJ/kg$ ]                          |
| $h_g$      | specific heat of vaporization [ $kJ/kg$ ]          |
| $Ja$       | Jacob number                                       |
| $L$        | length [ $m$ ]                                     |
| $\dot{m}$  | mass flux density [ $kg/m^2 s$ ]                   |
| $\dot{M}$  | mass flux [ $kg/s$ ]                               |
| $p$        | pressure [ $bar$ ]                                 |
| $\dot{q}$  | heat flux density [ $kJ/m^2 s$ ]                   |
| $Q$        | heat flux [ $kJ/s$ ]                               |
| $T$        | temperature [ $^{\circ}C$ ]                        |
| $\Delta T$ | subcooling [ $\Delta T = (T - T_s); K$ ]           |
| $U$        | circumference [ $m$ ]                              |
| $V_x$      | vapor drift velocity                               |
| $x$        | true quality                                       |
| $x_{eq}$   | equilibrium quality                                |
| $z$        | axial coordinate [ $m$ ]                           |

#### Greek Symbols

|                  |                               |
|------------------|-------------------------------|
| $\alpha$         | heat transfer coefficient     |
| $\epsilon$       | volumetric void fraction      |
| $\dot{\epsilon}$ | volumetric flow concentration |
| $\rho$           | density [ $kg/m^3$ ]          |
| $\sigma$         | surface tension [ $N/m$ ]     |

#### Subscripts

|         |                      |
|---------|----------------------|
| $c$     | critical             |
| $co$    | condensation         |
| $e, in$ | inlet                |
| $g$     | gas phase            |
| $heat$  | heated               |
| $l$     | liquid phase         |
| $ndp$   | net vapor production |

|        |                           |
|--------|---------------------------|
| $mc$   | micro-convection          |
| $rc$   | recondensation            |
| $s$    | saturation                |
| $sb$   | onset of nucleate boiling |
| $sp$   | single phase              |
| $theo$ | theoretical               |
| $tot$  | total                     |

#### REFERENCES

1. E. Mayinger, "Strömung und Wärmeübergang in Gas-Flüssigkeitsgemischen", Springer Verlag, Berlin, 1982.
2. G. E. Dix, "Vapor Void Fractions for Forced Convection with Subcooled Boiling at Low Flow Rates", Ph.D. thesis, Univ. of California, 1970.
3. P. K. Jain, K. Nourmohammadi, and R. Roy. "A Study of Forced Convective Subcooled Boiling in Heated Annular Channels", *NucEear Eng. Design*, vol. 60, 1980.
4. S. Z. Rouhani, "Calculation of Steam Volume Fraction in Subcooled Boiling", *Trans. ASME*, 1968.
5. G. Stängl, F. Mayinger "Void Fraction Measurement in Subcooled Forced Convective Boiling". *Exp. Heat Transfer Vol. 3 No. 3*. 1990
6. H. Bräuer, "Wärmeübergang und Siedebeginn bei unterkühltem Sieden unter Zwangskonvektion". *Diss. T.U. München*, 1988
7. N. Zuber and J. A. Findlay, "Average Volumetric Concentration in Two Phase Flow Systems", *J. Heat Transfer*, vol 87, 1975.
8. L. Friedel. "Modellgesetze für den Reibungsdruckverlust in der Zweiphasenströmung". *Diss. Univ. Hannover*, 1974.
9. Ulrych, G., "Strömungsvorgänge mit unterkühltem Sieden in Brennstabbindeln wassergekühlter Reaktoren". *Diss. T.U. Braunschweig* 1976
10. Huges, E. D., Paulsen, M. ; Agee, L. P. "A Drift Flux Model of Two Phase Flow". *A.S.M.E., Nuclear Technology, Vol 54*, 1981.
11. Rouhani, Z, Axelsson, E., "Calculation of Void Volume Fraction in the Subcooled and Quality Region". *Int. J. Heat and Mass Transfer Vol. 13*, pp. 383 - 393, 1970
12. Larson, P. S., Tong, L. S. "Void Fraction in Subcooled Boiling". *Heat Transfer Vol. 91*, pp. 472, 1969
13. Bowring, R. W. "Physical Model based on Bubble Detachment and Calculation of Steam Voidage in the Subcooled Region of a Heated Channel", *Institut for Atomenergie, Halden, Norway, HPR 10*, 1962
14. Han, C., Griffith, P., "The Mechanism of Heat Transfer in Nucleate Pool Boiling", Part I and II. *Int. j. Heat Mass Transfer, Vol. 8*, pp887 - 913, 1965